

Elucidation of Chiral Recognition Mechanism of α -Amino Acids using Ligand Exchange High Performance Liquid Chromatography

Jaqueline D. Senra,^{a,b} Luiz Fernando B. Malta,^a Patricia M. N. Ceva-Antunes,^a
Rodrigo J. Corrêa^{*a} and O. A. C. Antunes^{a,b}

^aInstituto de Química, UFRJ, CT Bloco A 641, Cidade Universitária,
21941-590 Rio de Janeiro-RJ, Brazil

^bNúcleo de Pesquisas de Produtos Naturais, UFRJ, CCS Bloco H, Cidade Universitária,
21941-590 Rio de Janeiro-RJ, Brazil

A técnica de HPLC por troca de ligante foi utilizada para a separação de racematos de amino ácidos com cadeia lateral alifática. Para tanto, o seletor quiral escolhido foi o complexo de Cu(II) combinado com a L-fenilalanina. Os resultados mostram que o primeiro enantiômero a eluir foi a forma D, seguido da forma L. Segundo o conceito de interação de 3 pontos, foi proposto um mecanismo de reconhecimento quiral, no qual não há evidências de mudança de configuração após a formação dos complexos pseudo-homo e heteroquiral. Cálculos DFT-B3LYP para energia e espectro vibracional confirmaram a viabilidade deste mecanismo, pois mostram a que a configuração trans do complexo homoquiral é mais estável do que a forma cis.

Ligand exchange HPLC technique was applied to resolve chiral separation of aliphatic side chain amino acid racemates. Chiral selector was copper L-phenylalaninate (II) and the results showed the elution of D enantiomer followed by L form. Considering the 3-point interaction concept, a mechanism of chiral recognition was proposed, in which no change of configuration would follow the formation of pseudo-homochiral and heterochiral complexes. To prove the reliability of this mechanism, the *trans* configuration of homochiral complex had to be more stable than the *cis* form, which was confirmed by DFT-B3LYP calculation in gas phase. The infrared frequencies were also calculated and the comparison with the subtracted and deconvoluted spectrum of the in-solution complex also pointed to the presence of the *trans* diastereoisomer.

Keywords: α -amino acids, L-phenylalanine, ligand exchange chromatography, *ab initio* molecular orbital calculations, fourier self-deconvolution

Introduction

Chiral separation has become an important and fascinating research field in the separation sciences since it was discovered that the chirality of molecules greatly affects their bioactivity. It has also been recognized that the analytical separation of α -amino acid enantiomers is of importance in research from the synthetic point of view up to the understanding of the origin of life. Recently separation scientists have focused their attention on the development of enantioseparation methods for α -amino acids in extraterrestrial exploration¹

and in situ analysis in space missions.² It is to be expected that the study on chirality, such as asymmetric synthesis and chiral separation, will play a more and more important role in life sciences, the pharmaceutical industry and other fields in the near future.

High Performance Liquid Chromatography (HPLC) has been one of the most important and flexible analytical tool in routine separations. However, the high costs of chiral columns and relatively short lifetime have lead to search resources such as the use of chiral additives added to mobile phase, which makes the use of achiral reversed phase material possible.

Ligand Exchange (LE), a mode of chiral discrimination, was introduced in liquid chromatography

*e-mail: rcorrea@iq.ufrj.br

in 1970 by Davankov and widely used for the enantioseparation of compounds such as amino acids, hydroxy acids and peptides.^{3,4} Based on the ligand exchange principle, chiral resolution is possible due to the transient formation of a pair of diastereomers, pseudo-homochiral and pseudo-heterochiral complexes, with different chemical properties and consequently different retentivities in the mobile phase.⁵⁻¹³

Our previous publication¹⁴ reported the successful study of three chiral selectors: L-proline, L-hydroxyproline and *N,N*-dimethyl-L-phenylalanine combined with Cu(II) ion in the mobile phase for the enantioseparations of some α -amino acids, with the elution order of D followed by L, using RP (Reversed Phase)-HPLC. In order to determine the preferable configuration of the diastereoisomeric complex (Figure 1), it was carried out for both isomers a theoretical study of structure optimization and infrared spectra simulation in the 100-600 cm^{-1} range, which corresponds to the bands assigned as metal-ligand vibrations. This was done to corroborate the mechanism proposed for the chiral recognition process, according to the concept of the 3-point interaction.¹⁵⁻¹⁷

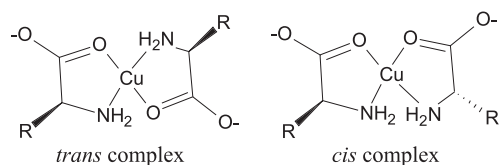


Figure 1. Possible homochiral complex diastereoisomers present in the mobile phase.

The aim of the present work is, therefore, to investigate the previous hypothesis about the mechanism of chiral recognition, studying the enantioseparation of valine, alanine, methionine and leucine optical isomers by using Ligand Exchange Liquid Chromatography with L-phenylalanine as the chiral selector and copper (II) as the central cation.

Results and Discussion

General chromatographic results

The enantioselectivities (α) and retention factors (k) were obtained for all racemic mixtures (Table 1). According to the α values obtained, all racemic mixtures were resolved, with D eluting before L (Figure 2).

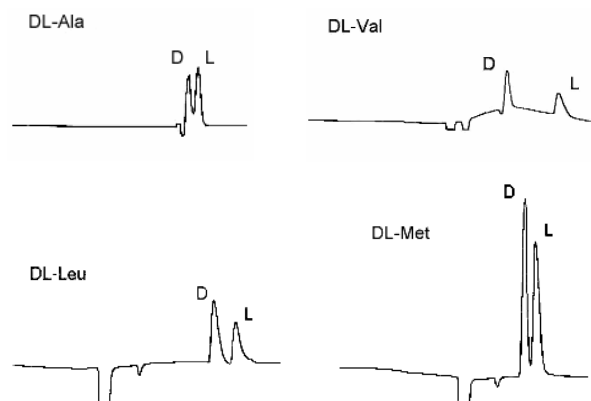


Figure 2. Enantioseparations of α -amino acids using Cu(II)-L-phenylalanine as chiral selector.

From these results, it is proposed the mechanism for the chiral recognition. In the lack of derivatization, the chiral liquid chromatography presume the formation of diastereoisomeric complexes, through ligand exchange, which is constrained by differences between equilibrium constants and rates of the ligand exchange reactions. When both of these factors are favoured chiral recognition happens. At this point, is important to emphasize the hydrophobic interactions in the stationary phase, which contribute decisively on selectivity.

The observed elution behaviour can give information about the chiral recognition mechanism. It shows that the L enantiomer is held tighter through

Table 1. Retention factors and enantioselectivity using L-phenylalanine as chiral selector in the mobile phase^a

α -amino acid	Water			5%(v/v) MeOH			15%(v/v) MeOH		
	k_D	k_L	α	k_D	k_L	α	k_D	k_L	α
Alanine (Ala)	0.18	0.26	1.44						
Valine (Val)				0.61	1.03	1.69			
Leucine (Leu)							1.00	1.18	1.18
Methionine(Met)							0.61	0.71	1.16

^aAnalysis conditions: column SUPELCOSIL LC-C18-DB; eluent, 1 mmol L^{-1} $\text{Cu}(\text{OAc})_2$ and 2 mmol L^{-1} of the chiral selector, resulting pH = 5, flow rate, 1.0 mL min^{-1} .

the stationary phase than the D form. This can be explained in terms of the possible different complex structures present in solution. Complex structures with R groups pointed “up” would interact better with the stationary phase than those pointed to opposite sides (Figure 3).

Then, the following situations are possible to happen: *i*) homochiral *trans* complex present in the mobile phase exchanges with L and D enantiomers, with greater retention of the L form, which does reproduce the experimental data; *ii*) homochiral *cis* complex present in the mobile phase exchanges with L and D enantiomers, with greater retention of the D form, which does not reproduce the experimental data.

These situations are related to structures with both R groups pointed “up” when the L and D forms are involved in the pseudo-homo and heterochiral complex formation, respectively (Figure 4). Then, to reproduce the chromatographic data, the homochiral *trans* complex must be more stable than the *cis* form. The main assumption here is that the R group does not influence the metal-ligand configuration. Therefore, the ligand exchange is not followed by a configuration change.

Experimental-theoretical study

An early study by Jackovitz and coworkers^{18,19} investigated similar complexes and their infrared spectra in the solid state and proposed the *trans* stereochemistry as the most stable. This model was exposed in our previous work of chiral recognition.¹⁴

In order to examine what configuration is thermodynamically favored, we have carried out theoretical studies with the two possible homochiral complex structures.

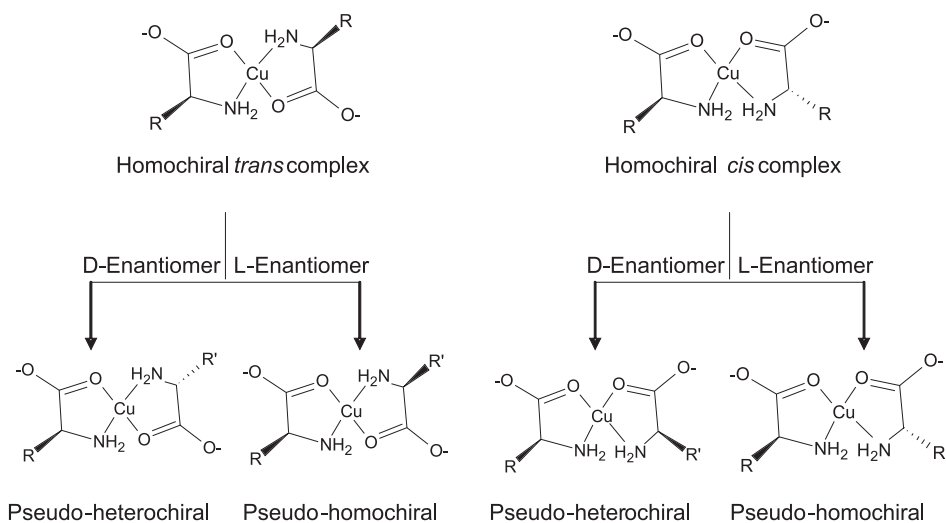


Figure 4.

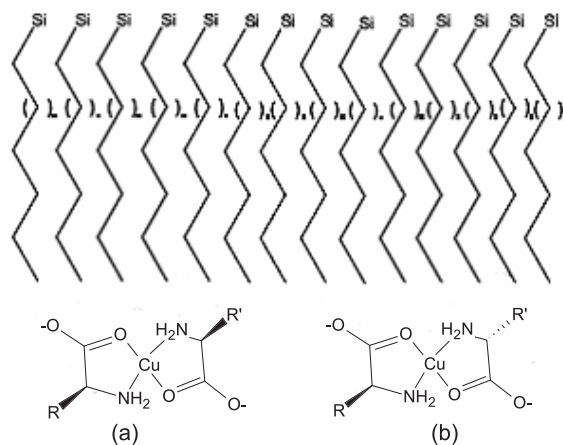


Figure 3. Scheme of C_{18} stationary phase interaction with (a) pseudo-homochiral and (b) heterochiral complexes.

DFT-B3LYP calculation was carried out for the *cis* and *trans* isomers in order to obtain their relative stabilities. From the structure optimization (Figure 5), the energy values for both diastereoisomers were used to evaluate the population quotient given by the Boltzmann distribution law:

$$\frac{N_{cis}}{N_{trans}} = e^{-\frac{\Delta E}{RT}}$$

where N_{trans} and N_{cis} are the numbers of *trans* and *cis* complexes; $\Delta E = E_{cis} - E_{trans}$, where E_{trans} and E_{cis} are: -1304.457 and -1304.437 Hartrees, respectively; $R = 8.3145$ Joule $\text{mol}^{-1} \text{K}^{-1}$; and $T = 298$ K. The energy barrier, ΔE , between the forms is of 52.0 kJ mol^{-1} . This gives a population quotient with largeness order of 10^{10} . It means that in-solution the homochiral complex is mostly the *trans* diastereoisomer.

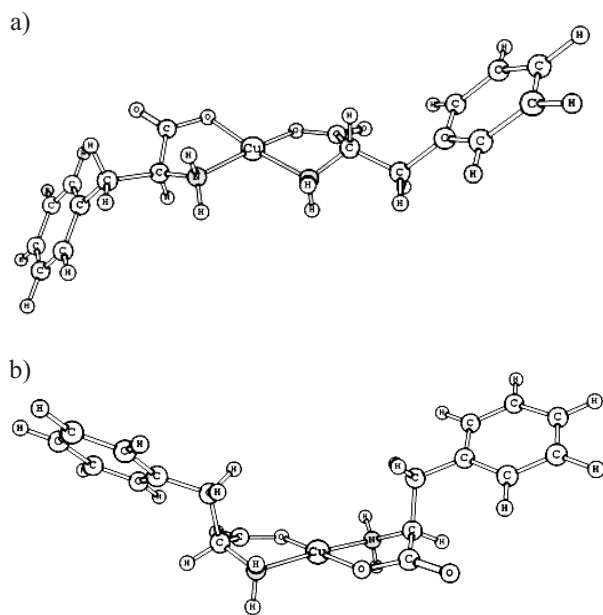


Figure 5. Optimized structures of the homochiral complex $[\text{Cu}(\text{L-C}_{18}\text{H}_{20}\text{N}_2\text{O}_4)_2]$ in the (a) *cis*; and (b) *trans* configurations.

Theoretical IR spectra were generated together with the structure optimization process. Both complex configurations have the same symmetry point group, C_{2v} , hence the number of bands given by each calculation was the

same. Both forms showed very similar spectra, and those were compared to experimental data obtained in the 100-600 cm^{-1} interval (Table 2 and 3). The experimental spectra was obtained using an aqueous solution of $\text{Cu}(\text{L-Phe})_2$. This signal was subtracted from those of the precursors, and the result was submitted to Fourier self-deconvolution. We applied this process in our previous study²⁰ and the assignment was successful. Table 2 and 3 show that the correlation produced mean discrepancies of 3-4% for both complex forms, which is a good agreement.

To determine which form was present in aqueous media, band intensities of the experimental spectrum were compared to those calculated for *cis* and *trans* complexes (Tables 4 and 5). As a reference value of intensity, it was chosen a band assigned as only ligand mode, *i.e.*, the highest intensity out-of-plane mode of phenyl C-H, at 406 cm^{-1} . This band is localized at 418 cm^{-1} in the experimental spectrum. To identify which calculated spectra had major agreement with the experimental one, the quotient $\frac{I_{cis \text{ or } trans}}{I_{406}}$ was compared

to $\frac{I_{exp}}{I_{418}}$ as showed in the last right column of Tables 4 and 5. The minor difference between these two quotients was obtained for the *trans* configuration, one order of magnitude

Table 2. Comparison between the observed and calculated vibrational frequencies (cm^{-1}) obtained by *ab initio* DFT/B3LYP calculation (predicted vibrational frequencies at the level 6-31G which have been scaled by a single factor of 0.9614) of the *trans*-Cu(L-Phe)₂

Mode assignment	Experimental	Theoretical	%
	$\nu/(\text{cm}^{-1})$	$\nu/(\text{cm}^{-1})$	
$\delta (\text{C}_2\text{C}_1\text{C}_6) + \delta (\text{COO}^-) + \delta (\text{NC}_a\text{C}_b)$	588	584	0.7
$\rho (\text{NH}_2) + \delta (\text{COO}^-) + \nu (\text{C}_a\text{-Cl}) + \delta (\text{CCC})_{\text{ring}} + \delta (\text{NC}_a\text{C}_b)$		578	1.7
$\text{o.p.} (\text{C}_{\text{ring}}\text{-H}) + \delta (\text{NC}_a\text{Cl}) + \tau (\text{NH}_2)$		530	9.9
$\text{o.p.} (\text{C}_{\text{ring}}\text{-H}) + \delta (\text{NC}_a\text{Cl}) + \tau (\text{NH}_2)$		523	11.0
$\text{o.p.} (\text{C}_{\text{ring}}\text{-H}) + \nu (\text{Cu-N})_{\text{asym}} + \delta (\text{NC}_a\text{C}_b) + \rho (\text{NH}_2) + \omega (\text{COO}^-)$	459	475	3.5
$\text{o.p.} (\text{C}_{\text{ring}}\text{-H}) + \delta (\text{NC}_a\text{Cl}) + \omega (\text{COO}^-)$		472	2.8
$\nu (\text{Cu-N})_{\text{asym}}$		452	1.5
$\rho (\text{HC}_a\text{N}) + \nu (\text{Cu-N})_{\text{asym}} + \rho (\text{COO}^-)$	434	432	0.5
$\text{o.p.} (\text{C}_{\text{ring}}\text{-H})$	418	406	2.9
		406	2.9
$\nu (\text{Cu-N})_{\text{asym}} + \nu (\text{Cu-O})_{\text{asym}}$	395	402	1.8
$\rho (\text{CH}_2) + \omega (\text{COO}^-)$	369	352	4.6
$\rho (\text{CH}_2) + \rho (\text{HC}_a\text{N}) + \rho (\text{COO}^-) + \delta (\text{C}_a\text{NCu})$	349	350	0.3
$\rho (\text{NH}_2) + \rho (\text{CH}_2) + \delta (\text{C}_a\text{C}_b\text{C}_1)$		342	2.0
$\rho (\text{NH}_2) + \omega (\text{CuNC}_a)$		330	1.9
$\rho (\text{NH}_2) + \rho (\text{CH}_2) + \tau (\text{C}_b\text{C}_a\text{N})$	324	300	0.7
$\nu (\text{Cu-N})_{\text{asym}} + \nu (\text{Cu-O})_{\text{sym}}$	270	284	5.2
$\delta (\text{OCuN}) + \rho (\text{CH}_2)$	249	250	0.4
$\text{o.p.} (\text{Cl-C}_b) + \rho (\text{CH}_2)$	206	226	9.7
$\omega (\text{OCuO}) + \omega (\text{NCuN}) + \text{o.p.} (\text{Cl-C}_b)$		197	4.4
$\omega (\text{COO}^-) + \rho (\text{NH}_2) + \omega (\text{NC}_a\text{C}_b)$		190	7.8
$\omega (\text{OCuO}) + \omega (\text{NCuN})$	187	186	0.5
			Mean % = 3.5

I = intensities (in Debye units). Approximate description of assignments: ν \rightarrow stretching; δ \rightarrow bending; ω \rightarrow wagging; ρ \rightarrow rocking; sym \rightarrow symmetric; asym \rightarrow asymmetric; i.p. \rightarrow in-plane; o.p. \rightarrow out-of-plane; C1 \rightarrow substituted ring carbon.

Table 3. Comparison between the observed and calculated vibrational frequencies (cm^{-1}) obtained by *ab initio* DFT/B3LYP calculation (predicted vibrational frequencies at the level 6-31G which have been scaled by a single factor of 0.9614) of the *cis*-Cu(L-Phe)₂

Mode assignment	Experimental	Theoretical	%
	$\nu(\text{cm}^{-1})$	$\nu(\text{cm}^{-1})$	
$\rho(\text{NH}_2) + \omega(\text{COO}^-) + \delta(\text{C}_2\text{C}_b\text{C}_a) + \text{o.p.}(\text{C}_{\text{ring}}-\text{H})$	588	584	0.7
$\rho(\text{NH}_2) + \delta(\text{COO}^-) + \delta(\text{C}_2\text{C}_1\text{C}_6) + \text{i.p.}(\text{C}-\text{H})$		584	0.7
$\rho(\text{NH}_2) + \omega(\text{COO}^-) + \delta(\text{C}_2\text{C}_1\text{C}_6)$		580	1.4
$\delta(\text{C}_b\text{C}_a\text{N}) + \delta(\text{COO}^-) + \delta(\text{C}_2\text{C}_1\text{C}_6) + \nu(\text{Cu-O})_{\text{asym}}$		572	2.7
$\text{o.p.}(\text{C}_{\text{ring}}-\text{H}) + \delta(\text{C}_a\text{CN}) + \rho(\text{NH}_2)$		534	9.2
$\text{o.p.}(\text{C}_{\text{ring}}-\text{H}) + \delta(\text{NH}_2)$		533	9.4
$+ \delta(\text{C}_a\text{CN}) + \delta(\text{C}_a\text{CO}) + \nu(\text{Cu-O})_{\text{asym}} + \nu(\text{Cu-N})_{\text{asym}}$			
$\text{o.p.}(\text{C}_{\text{ring}}-\text{H}) + \nu(\text{Cu-N})_{\text{sym}} + \rho(\text{COO}^-)$	459	475	3.5
$\text{o.p.}(\text{C}_{\text{ring}}-\text{H}) + \nu(\text{Cu-N})_{\text{asym}} + \rho(\text{COO}^-)$		469	2.2
$\text{o.p.}(\text{C}_{\text{ring}}-\text{H}) + \nu(\text{Cu-N})_{\text{sym}} + \rho(\text{NH}_2)$	434	449	3.4
$\text{o.p.}(\text{C}_{\text{ring}}-\text{H}) + \tau(\text{HC}_a\text{N}) + \nu(\text{Cu-N})_{\text{asym}}$		446	2.8
$+ \nu(\text{CuO})_{\text{asym}}$			
$\text{o.p.}(\text{C}_{\text{ring}}-\text{H})$	418	406	2.9
		406	2.9
$\text{o.p.}(\text{C}_{\text{ring}}-\text{H}) + \nu(\text{Cu-O})_{\text{sym}} + \nu(\text{Cu-N})_{\text{sym}} + \omega(\text{COO}^-) + \rho(\text{COO}^-)$	395	385	2.5
$\rho(\text{CH}_2) + \omega(\text{C}_2\text{C}_b\text{C}_a) + \rho(\text{COO}^-) + \nu(\text{Cu-O})_{\text{sym}} + \nu(\text{Cu-N})_{\text{sym}}$	369	346	6.2
$\rho(\text{CH}_2) + \rho(\text{NH}_2) + \omega(\text{C}_1\text{C}_b\text{C}_a)$	349	339	2.9
$\rho(\text{CH}_2) + \rho(\text{NH}_2) + \omega(\text{C}_1\text{C}_b\text{C}_a) + \omega(\text{COO}^-) + \nu(\text{Cu-O})_{\text{asym}}$		338	1.8
$\text{o.p.}(\text{C}_{\text{ring}}-\text{H}) + \rho(\text{CH}_2) + \rho(\text{C}_a\text{C}_b\text{N})$	324	324	2.4
$\rho(\text{CH}_2) + \rho(\text{NH}_2) + \omega(\text{C}_a\text{C}_b\text{N}) + \nu(\text{Cu-O})_{\text{sym}}$	298	297	0.3
$\text{o.p.}(\text{C}_{\text{ring}}-\text{H}) + \rho(\text{CH}_2) + \rho(\text{NH}_2) + \omega(\text{COO}^-)$	270	261	3.4
$\text{o.p.}(\text{C}_{\text{ring}}-\text{H}) + \rho(\text{CH}_2) + \rho(\text{NH}_2)$	249	250	0.4
$\delta(\text{C}_1\text{C}_b\text{C}_a) + \tau(\text{CH}_2)$	206	212 212	2.9
			2.9
$\omega(\text{OCuO}) + \omega(\text{NCuN})$	187	183	2.1
			Mean % = 3.1

I = intensities (in Debye units). Approximate description of assignments: ν → stretching; δ → bending; ω → wagging; ρ → rocking; sym → symmetric; asym → asymmetric; i.p. → in-plane; o.p. → out-of-plane; C1 → substituted ring carbon.

Table 4. Comparison between intensity quotients of experimental and theoretical *trans* spectra

Theoretical		Experimental		$\frac{I_{\text{exp}}}{I_{418}}$	$\frac{I_{\text{trans}}}{I_{406}}$	$\left(\frac{I_{\text{exp}}}{I_{418}} - \frac{I_{\text{trans}}}{I_{406}}\right)^2$
$\nu(\text{cm}^{-1})$	I_{trans}	$\nu(\text{cm}^{-1})$	I_{exp}			
584	10.14	588	0.48	0.786885	7.140845	40.37281
578	1.8		0.48	0.786885	1.267606	0.231092
530	40.44		0.48	0.786885	28.47887	766.8462
523	16.55		0.48	0.786885	11.65493	118.1144
475	21.04	459	0.1	0.163934	14.8169	214.7094
472	7.32		0.1	0.163934	5.15493	24.91003
452	24.61		0.1	0.163934	17.33099	294.7077
432	0.61	434	0.74	1.213115	0.429577	0.613931
406	1.42	418	0.61	1	1	0
406	0.45		0.61	1	0.316901	0.466624
402	55.38	395	0.26	0.42623	39	1487.936
352	2.85	369	0.39	0.639344	2.007042	1.870598
350	11.83	349	0.48	0.786885	8.330986	56.91345
342	0.16	324	0.2	0.327869	0.112676	0.046308
330	1.3		0.2	0.327869	0.915493	0.345302
300	18.43	298	0.32	0.52459	12.97887	155.1092
284	0.38	270	1.12	1.836066	0.267606	2.460067
250	0.2	249	0.91	1.491803	0.140845	1.825088
226	0.64	206	0.75	1.229508	0.450704	0.606536
197	22.08		0.75	1.229508	15.5493	205.0563
190	5.21		0.75	1.229508	3.669014	5.951189
186	0.38	187	1.16	1.901639	0.267606	2.670066
Mean $\left(\frac{I_{\text{exp}}}{I_{418}} - \frac{I_{\text{trans}}}{I_{406}}\right)^2 = 153.7165$						

lower than that for the *cis* form (Tables 4 and 5). Hence this result corroborated the energy result of DFT calculation in gas phase, which gave the *trans* isomer as the most stable.

Experimental

Chemicals

DL-alanine, DL-valine, DL-leucine, DL-methionine and L-phenylalanine were obtained from Sigma (St. Louis, MO, USA); methanol (HPLC-grade) was from Tedia Brasil (Rio de Janeiro, RJ, Brazil); copper(II) acetate was from Merck (Darmstadt, Germany).

Instrumentation

A Shimadzu LC-10AS high performance liquid chromatograph (Shimadzu, Japan), equipped with a Rheodyne model 7125 injection valve, was used and coupled to a Supelcosil LC-C18 DB column (250 mm \times 4.6 mm), from Supelco (Bellefonte, PA, USA), with 5 μ m particle size and 10 nm pore diameter. Photometric detection was used at 254 nm (variable wavelength UV detector Shimadzu SPD-10AV).

Water was purified with an Ultra Pure System-Milli-Q Plus from Millipore™ (Bedford, MA, USA).

Sample preparation for HPLC analysis

Racemic mixtures

Aqueous solutions of the enantiomeric mixtures and of the L and D-isomers of the α -amino acids were prepared with a final concentration of 0.5 mg mL⁻¹. These solutions were filtered through an Iso-Disc N-34 nylon membrane (0.45 μ m \times 3 mm) from Supelco and analysed several times. In order to determine the column void time, it was used a solution of sodium nitrate, which gave $t_M = 3.4$ min.

Preparation of the chiral mobile phase

L-phenylalanine (2 mmol L⁻¹) and Cu(CH₃COO)₂ (1 mmol L⁻¹) were dissolved in Milli-Q water or Milli-Q water/methanol. The final measured pH was 5.0. These solutions were filtered through Nylon 66 membranes (0.2 mm \times 47 mm) from Supelco. The system was equilibrated with the mobile phase until the detector base line was stabilized and, therefore, zeroed.

FTIR characterization

Homochiral complex of copper with L-phenylalanine, Cu(L-Phe)₂, was obtained in solution by mixing of

Table 5. Comparison between intensity quotients of experimental and theoretical *cis* spectra

Theoretical		Experimental		$\frac{I_{\text{exp}}}{I_{418}}$	$\frac{I_{\text{trans}}}{I_{406}}$	$\left(\frac{I_{\text{exp}}}{I_{418}} - \frac{I_{\text{trans}}}{I_{406}}\right)^2$
$\nu/(\text{cm}^{-1})$	I_{trans}	$\nu/(\text{cm}^{-1})$	I_{exp}			
584	6.15	588	0.48	0.786885	10.25	89.55054
584	5.54		0.48	0.786885	9.233333	71.34249
580	0.8		0.48	0.786885	1.333333	0.298606
572	5.53		0.48	0.786885	9.216667	71.06121
534	1.26		0.48	0.786885	2.1	1.72427
533	63.83		0.48	0.786885	106.3833	11150.61
475	2.04	459	0.1	0.163934	3.4	10.47212
469	28.82		0.1	0.163934	48.03333	2291.479
449	0.29	434	0.74	1.213115	0.483333	0.532581
446	57.17		0.74	1.213115	95.28333	8849.206
406	0.06	418	0.61	1	0.1	0.81
406	0.6		0.61	1	1	0
385	1.44	395	0.26	0.42623	2.4	3.89577
346	6.54	369	0.39	0.639344	10.9	105.2811
339	9.58	349	0.48	0.786885	15.96667	230.4258
338	8.13		0.48	0.786885	13.55	162.8971
324	59.4	324	0.2	0.327869	99	9736.189
297	0.31	298	0.32	0.52459	0.516667	6.28E-05
261	0.95	270	1.12	1.836066	1.583333	0.063874
250	10.82	249	0.91	1.491803	18.03333	273.6222
212	5.79	206	0.75	1.229508	9.65	70.90468
212	3.84		0.75	1.229508	6.4	26.73399
183	0.54	187	1.16	1.901639	0.9	1.003281

$$\text{Mean} \left(\frac{I_{\text{exp}}}{I_{418}} - \frac{I_{\text{cis}}}{I_{406}} \right)^2 = 1441.222$$

precursors in order to give a 2 mmol L⁻¹ solution. This complex was analyzed by FTIR spectroscopy using a Nicolet Magma spectrometer with 4 cm⁻¹ resolution and 64 accumulations. The sample was prepared by producing a liquid film in polyethylene matrix. Data were collected in the 100-600 cm⁻¹ interval. The FTIR signal of the complex was subtracted from those of copper acetate and L-phenylalanine solutions in appropriate concentrations and deconvoluted. OMNIC XP software was used for this mathematical procedure.

Ab initio calculation

The geometry of several species were optimized using standard techniques²¹ and, after geometry optimization, vibrational analysis was performed and the resulting geometries were checked with respect of being true minima on the potential energy surface, as shown by the absence of imaginary frequencies. Geometrical, energetic and vibrational analysis were performed at UB3LYP/6-311++G**//UB3LYP/6-31G* with lanl2dz for Cu atom.

Conclusions

The previously proposed mechanism of chiral recognition of α -aminoacids using copper L-phenylalaninate (II) chiral selector in ligand exchange HPLC was supported by DFT-B3LYP calculation carried out in the present paper. To justify the experimental elutions of D and L forms, the *trans* configuration of homochiral complex had to be more stable than the *cis* form. This was confirmed by DFT-B3LYP calculation in gas phase, with an energy barrier of 8.7189×10^{-20} Joule per molecule between the two forms. The infrared frequencies were also calculated and the comparison by means of intensity quotients with the subtracted and deconvoluted spectrum of the in-solution complex also pointed to the presence of the *trans* diastereoisomer.

Acknowledgments

The authors would like to thank FAPERJ, CAPES and CNPq (Brazil) for financial support; and Mr. Glaucio Braga Ferreira for the helpful comments in the present work.

References

1. Hutt, L.D.; Glavin, D.P.; Bada, J.L.; Mathies, R.A.; *Anal. Chem.* **1999**, *71*, 4000.
2. Rodier, C.; Laurent, C.; Coscia, D.; Sterner, L.; Raulin, F.; Vidal-Madjar, C.; *Abstract of 13th ISCD (Chirality 2001)*, P-232, Orlando, USA, July 15-18, 2001.
3. Davankov, V. A.; Rogozhin, S.V.; *J. Chromatogr.* **1971**, *60*, 280.
4. Davankov, V. A.; Navratil, J.D.; Walton, H.F.; *Ligand Exchange Chromatography*, CRC Press: Boca Raton, FL, 1988.
5. Gilon, C.; Leshem, R.; Grushka, E.; *Anal. Chem.* **1980**, *52*, 1206.
6. Davankov, V. A.; Kurganov, A.A.; *Chromatographia* **1983**, *17*, 686.
7. Wernicke, R.; *J. Chromatogr. Sci.* **1985**, *23*, 39.
8. Pirkle, W.H.; Pochapsky, T.C.; *Chem. Rev.* **1989**, *89*, 347.
9. Galaverna, G.; Corradini, R.; DeMunari, E.; Dossena, A.; Marchelli, R.; *J. Chromatogr. A* **1993**, *657*, 43.
10. Husain, S.; Sekar, R.; Rao, R.N.; *J. Chromatogr. A* **1994**, *687*, 351.
11. Galaverna, G.; Corradini, R.; Dossena, A.; Chiavaro, E.; Marchelli, R.; Dallavalle, F.; Folesani, G.; *J. Chromatogr. A* **1998**, *829*, 101.
12. Chen, Z.; Niitsuma, M.; Uchiyama, K.; Hobo, T.; *J. Chromatogr. A* **2003**, *990*, 75.
13. Rombach, M.; Gelinsky, M.; Vahrenkamp, H.; *Inorg. Chim. Acta* **2002**, *334*, 25.
14. Nazareth, P.M.P.; Antunes, O.A.C.; *J. Braz. Chem. Soc.* **2002**, *13*, 658.
15. Davankov, V.A.; *J. Chromatogr. A* **1994**, *666*, 55.
16. Pirkle, W.H.; *Chirality* **1997**, *9*, 103.
17. Hyun, M.H.; Ryoo, J.J.; Pirkle, W.H.; *J. Chromatogr. A* **2000**, *886*, 47.
18. Jackovitz, J.F.; Durkin, J.A.; Walter, J.L.; *Spectrochim. Acta A* **1967**, *23*, 67.
19. Jackovitz, J.F.; Walter, J.L.; *Spectrochim. Acta A* **1966**, *22*, 1393.
20. Malta, L.F.B.; Senra, J.D.; Medeiros, M.E.; Antunes, O.A.C.; *Supramol. Chem.* **2006**, *18*, 327.
21. Fletcher, R.; *Practical Methods of Optimization*, Wiley: New York, 1980, v.1.

Received: January 10, 2007

Web Release Date: November 12, 2007